Pattern Revivals from Fractional Gouy Phases in Structured Light

B. Pinheiro da Silva,[1] V. A. Pinillos,[2] D. S. Tasca,[1] L. E. Oxman,[1] and A. Z. Khoury[1,*]
[1]Instituto de Física, Universidade Federal Fluminense, 24210-346 Niterói, Rio de Janeiro, Brasil
[2]Departamento de Ciencias, Pontificia Universidad Católica del Perú, Apartado 1761, Lima, Perú

(Received 26 July 2019; revised manuscript received 25 October 2019; published 23 January 2020)

We investigate pattern revivals in specially designed optical structures that combine different transverse modes. In general, the resulting pattern is not preserved under free propagation and gets transformed due to nonsynchronized Gouy phases. However, it is possible to build structures in which the Gouy phases synchronize at specific fractional values, thus recovering the initial pattern at the corresponding longitudinal positions. This effect is illustrated with a radially structured light spot in which the beam energy can be addressed to different positions without the need of intermediate optical components, which can be useful for optical communications and optical tweezing with structured beams.

DOI: 10.1103/PhysRevLett.124.033902

The transverse structure of optical beams has been widely used for encoding information both in the classical and quantum domains [1,2]. Transmission and amplification of images and patterns either in free space or in optical resonators is still an active research area. In a multimode regime, the spatial structure of nonlocal quantum correlations gives rise to interesting and counterintuitive effects such as the so-called *ghost images* [3–14]. When few spatial modes are involved, they can serve as a finite dimension Hilbert space for encoding quantum information [15–17].

Within the limits of the paraxial approximation, an arbitrary spatial structure can be expanded in the well-known Hermite-Gaussian (HG) or Laguerre-Gaussian (LG) bases that are orthonormal solutions of the paraxial wave equation. Apart from a transverse rescaling due to diffraction, the intensity patterns associated to these solutions preserve their shape along free space propagation. However, their phase evolution depends on the mode parameters so that intensity patterns composed by different paraxial modes may not preserve their shape in free space propagation. In this regard, the Gouy phase plays a crucial role affecting the relative phase among the modes taking part in the pattern superposition. For example, this can lead to self-rotating patterns when different orbital angular momenta are combined in the mode superposition, as studied in Refs. [18,19].

Free propagation of spatially modulated beams leads to surprising features such as the well-known Talbot effect first noticed by Henry Fox Talbot in the nineteenth century [20]. He noticed that the spatial modulation imposed by a diffraction grating would periodically reproduce itself in the near field pattern. This effect has been also realized in matter waves [21]. Its origin relies on a periodic synchronization of the individual phase factors that figure on the contribution from each slit to the propagated field distribution. Interestingly, this kind of pattern revival also appears in atomic physics, where a localized electronic wave packet normally spreads with time. However, under special conditions, the spreading reverses itself and the wave packet recovers localization. The long-term evolution of a radially localized electronic wave packet formed by the coherent superposition of Rydberg states of atomic potassium has been demonstrated in Ref. [22]. A closely related decay and revival of coherence was predicted and observed in the micromaser realization of the Jaynes-Cummings model [23–26].

Nondiffracting and self-imaging beams have been investigated for a long period due to their potential applications in microscopy, microfabrication, and optical tweezing [27,28]. These beams can be engineered by suitably shaping the transverse Fourier spectrum of the light field, allowing the preparation of nondiffracting Bessel beams and projection of a given image to a desired position in space [29]. In this work, we implement pattern revivals with a suitable superposition of discrete paraxial modes in which the Gouy phases synchronize at specific longitudinal positions. The occurrence of these revivals is related to fractional Gouy phases determined by the mode orders. We exploit radially structured Laguerre-Gaussian modes to construct a self-restoring spot that can be used as the basic unit of a more complex pattern. This can be useful in different contexts, including optical imaging, tweezing, and quantum information platforms. The present work fits within an emerging line of work on manipulating beams of light, such as Bessel and Airy beam superpositions [30].

Free space propagation of optical beams in paraxial regime can be described by two-dimensional (2D) HG or LG functions. The HG basis for a beam with wave number k propagating along the z axis reads

$$u_{mn}(x,y,z) = X_m(x,z)Y_n(y,z)e^{-i\phi_N(z)}, \qquad (1)$$

where the Gouy phase

$$\phi_N(z) = (m+n+1)\arctan(z/z_0) \tag{2}$$

depends on the mode order $N = m + n$ and the Rayleigh parameter z_0 characterizing the diffraction distance. The mode functions are of the form

$$F_m(\xi, z) = \frac{\mathcal{N}_m}{\sqrt{w}} e^{-\left[\frac{ik\xi^2}{2R} + \frac{\xi^2}{w^2}\right]} H_m\left(\frac{\xi\sqrt{2}}{w}\right), \tag{3}$$

where $F = X,\ Y$, $\xi = x,\ y$, and $H_m(\xi)$ is the Hermite polynomial of order m. The normalization constant $\mathcal{N}_m$, the wave-front radius $R(z)$, and the beam width $w(z)$ are given by

$$\mathcal{N}_m = \frac{(2/\pi)^{1/4}}{2^{m/2} m!}, \tag{4}$$

$$R(z) = \frac{z_0^2 + z^2}{z}, \tag{5}$$

$$w(z) = \left(\frac{2(z_0^2 + z^2)}{k z_0}\right)^{1/2}. \tag{6}$$

The origin of the z axis is placed on the focal plane where the beam width is minimal and the wave front is plane ($R \to \infty$).

In cylindrical coordinates, paraxial modes can be expanded in the LG basis,

$$v_{pl}(r, \theta, z) = R_{pl}(r, z) e^{il\theta} e^{-i\phi_N(z)}, \tag{7}$$

where the Gouy phase now reads

$$\phi_N(z) = (2p + |l| + 1)\arctan(z/z_0), \tag{8}$$

and the mode order is $N = 2p + |l|$. The radial function is given by

$$R_{pl}(r, z) = \frac{\mathcal{N}_{pl}}{w}\left(\frac{r\sqrt{2}}{w}\right)^{|l|} L_p^{|l|}\left(\frac{2r^2}{w^2}\right) e^{-\left[\frac{ikr^2}{2R} + \frac{r^2}{w^2}\right]}, \tag{9}$$

where $L_p^{|l|}$ are generalized Laguerre polynomials and the normalization constant is

$$\mathcal{N}_{pl} = \left(\frac{2p!}{\pi(p + |l|)!}\right)^{1/2}. \tag{10}$$

Let us consider a normalized pattern composed by d basic structures with different orders $N_1, N_2, \ldots, N_d$,

$$\psi(\mathbf{r}) = \sum_{j=1}^{d} A_j \varphi_j(\mathbf{r}) e^{-i\phi_{N_j}(z)}. \tag{11}$$

Each basic structure $\varphi_j(\mathbf{r})$ can be a combination of HG, LG, or both kinds of modes sharing the same order N_j. Apart from diffraction, each basic structure evolves with a stable pattern and acquires a Gouy phase $\phi_{N_j}(z)$. Because of the different mode orders present in the superposition, the Gouy phases will evolve at different rates and ψ will not keep the original pattern along propagation. However, the pattern prepared at $z = 0$ may be repeated if all Gouy phases resynchronize along propagation, that is, if

$$\phi_{N_{j+1}}(z) - \phi_{N_j}(z) = 2q_j\pi (q_j \in \mathbb{Z}). \tag{12}$$

For a nonastigmatic beam in free space, this will occur at specific positions, but due to the limited range of the Gouy phase, not all multiples can be achieved.

In order to derive the exact location of the revivals, we first write

$$\psi_d(\mathbf{r}) = e^{-i\bar{\phi}(z)} \sum_{j=1}^{d} A_j \varphi_j(\mathbf{r}) e^{-i\Delta_j(z)}, \tag{13}$$

where

$$\bar{\phi}(z) = \frac{1}{d}\sum_{j=1}^{d} \phi_{N_j}(z), \tag{14}$$

$$\Delta_j(z) = \phi_{N_j}(z) - \bar{\phi}(z). \tag{15}$$

Note that $\sum_j \Delta_j = 0$, so that the phasors $e^{-i\Delta_j}$ form a diagonal $SU(d)$ matrix evolving along the beam propagation. A revival will occur when these phasors get aligned and this matrix structure becomes proportional to the identity, which can only happen with fractional phase factors since the evolution is closed in $SU(d)$ [31]. To see this more explicitly, we can use Eqs. (12) and (15) to arrive at the fractional phase condition

$$\sum_{j=1}^{d} \Delta_j = d\Delta_1 + 2\pi \sum_{j=2}^{d}\sum_{k=1}^{j-1} q_k = 0,$$
$$\Rightarrow \Delta_j = \frac{2\pi r_j}{d} \quad (r_j \in \mathbb{Z}), \tag{16}$$

where $r_1 = -\sum_{k=1}^{d-1}(d-k)q_k$ and $r_{j+1} = r_j + 2dq_j$. Therefore, revivals can only be obtained when the fractional phase condition (16) is fulfilled.

Going back to Eq. (12), we obtain the revival positions from

$$(N_{j+1} - N_j)s(z) = 4q_j, \tag{17}$$

where $s(z) \equiv (2/\pi)\arctan(z/z_0)$. Note that as one moves from the focal plane ($z = 0$) to the far field region ($z \to \infty$)

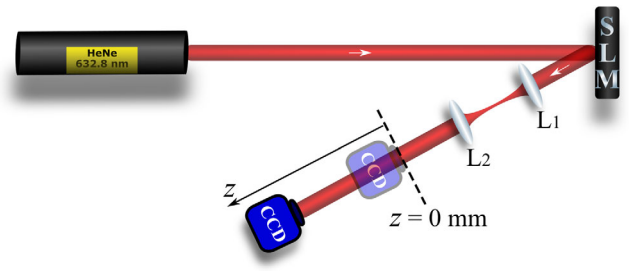

FIG. 1. Experimental setup.

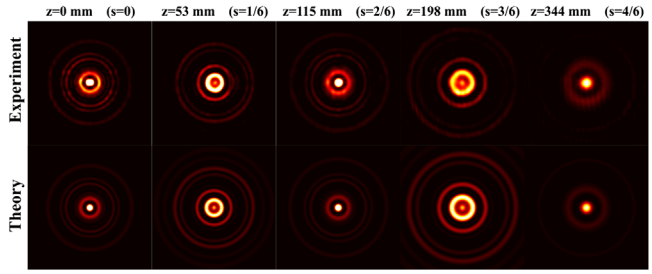

FIG. 2. Measured (top) and calculated (bottom) intensity distribution of the structure given by Eq. (19) at different planes along propagation.

the parameter s varies continuously between 0 and 1. In practice, the far field configuration can be approximately observed at distances $z \gg z_0$, that corresponds to $s \sim 1$.

Revivals require a minimum value ($N_{j+1} - N_j \geq 4$) for nonvanishing gaps between consecutive mode orders, except for the trivial situation in which $N_{j+1} = N_j$, corresponding to a pattern composed by modes of the same order that remain in phase along propagation. In the general case, for a given set of modes present in the superposition, the first revivals always occur at the position where $4/s(z)$ reaches the greatest common divisor $D(N_2 - N_1, \ldots, N_d - N_{d-1})$ of all nonvanishing mode gaps. Then, other revivals occur at the positions corresponding to the submultiples of D, reachable within the limits imposed on s. If the mode gaps do not have a common divisor greater than one, then revivals never occur, since it would imply the nonphysical condition $s = 4$. At the revival positions, the field distribution becomes

$$\psi_d(\bar{x}, \bar{y}, z) = e^{i\bar{\phi}(z)} e^{\frac{2i\pi r}{d}} \psi_d(\bar{x}, \bar{y}, 0), \tag{18}$$

where $\bar{x} = x/w(z)$, $\bar{y} = y/w(z)$, and $r = \min_j |r_j|$.

We now present some interesting numerical examples and the corresponding experimental results supporting our theoretical predictions. We demonstrated the revival effect with the setup shown in Fig. 1. A Gaussian beam from a He-Ne laser is sent to a spatial light modulator (SLM) programmed to produce the desired mode superposition. The screen of the SLM is imaged to a remote position with a pair of lenses (L1 and L2) to allow acquisition of the initial image with a charge-coupled device (CCD) camera. Then, the CCD is translated along the propagation axis z, starting from the screen image position $z = 0$.

Many different examples can be produced illustrating the revival effect based on fractional Gouy phases. We have observed this in different length scales from a few millimeters to a few meters. First, we will focus our demonstration on a superposition of three radial LG modes that define a bright spot at the focal plane and distributes its energy along propagation. The bright spot gets restored at the fractional Gouy phase positions. The effect is illustrated with the following three-mode structure,

$$\psi_3(\mathbf{r}) = 0.3 v_{0,0}(\mathbf{r}) + v_{6,0}(\mathbf{r}) + v_{12,0}(\mathbf{r}), \tag{19}$$

carrying $l = 0$ and $p = 0, 6, 12$. The mode gaps involved in the structure given in (19) are $N_2 - N_1 = N_3 - N_2 = 12$, whose denominators are $D = 1, 2, 3, 4, 6, 12$. The revival positions are determined by $s(z_j) = 4/D_j$ within the interval $0 \leq s \leq 1$. This results in $s(z_1) = 1/3$, $s(z_2) = 2/3$, and $s(z_3) = 1$, the last one corresponding to $z_3 \to \infty$. Normalization is irrelevant to our analysis. The relative weights of the radial modes were optimized to concentrate the intensity in the central spot, resulting in the distribution shown in the first picture of either the top (experiment) or bottom (theory) row in Fig. 2 where an intense central spot is surrounded by weak rings. As the beam propagates, this structure evolves and the intensity gets transversely redistributed as shown by the experimental results given in the top row of Fig. 2 and confirmed by the theoretical results shown in the bottom row of Fig. 2. We have also included the Supplemental Material [32] with an animation of the structured spot evolution and the geometric representation of the Gouy phase variation, showing synchronization at the revival positions.

As a striking illustration of the revival effect, we used the SLM to implement a set of structured spots given by Eq. (19), centered at different locations disposed to form the initials Universidade Federal Fluminense (UFF). The initial pattern is displayed at the top row in Fig. 3. Then,

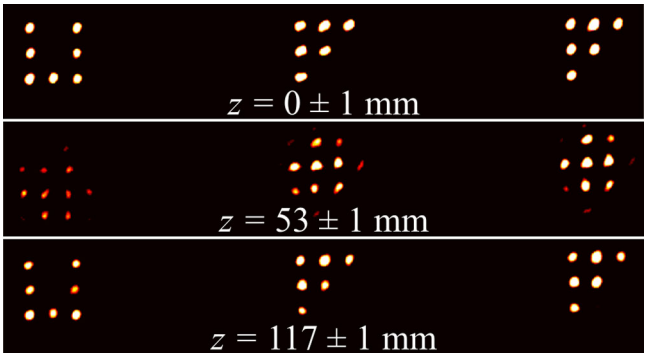

FIG. 3. Propagation sequence of the structured spot pattern forming the initials UFF. Three propagation planes are displayed: $z = 0$ (top), 53 mm (middle), and 117 mm (bottom). A revival is evident at 117 mm.

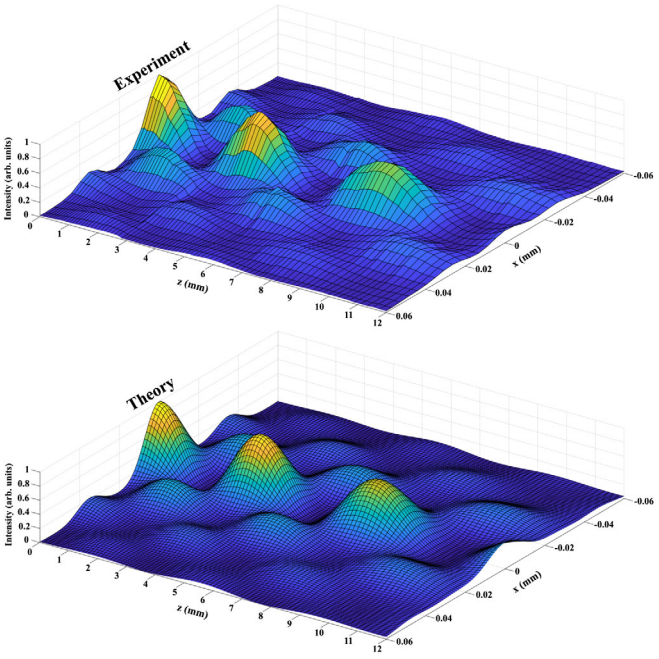

FIG. 4. 3D plot of the intensity distribution along a beam diameter at different propagation planes for the structured spot given by Eq. (20). The experimental result is displayed at the top graph and the theoretical calculation is shown at the bottom. Two revivals can be clearly seen, the first one located at 3.55 mm and the second one at 8.00 mm.

this pattern gets scrambled at intermediate longitudinal positions, until it gets restored at the revival position around 117 mm, where the Gouy phases get synchronized at the fractional phase differences. In order to improve the pattern visibility, we have applied a uniform step filter that cuts out the illumination caused by the weak external rings and the background light. We have also filmed the pattern evolution along propagation from the initial position until the first revival. The experimental videos are provided in the Supplemental Material [32] (raw images and noise filtered images).

In order to show that this effect can be useful for optical tweezing in the short distance range, we have also tested the pattern revival in the millimeter length scale. For this end, we have used the superposition

$$\psi_{\text{short}}(\mathbf{r}) = v_{0,0}(\mathbf{r}) + v_{12,0}(\mathbf{r}), \tag{20}$$

with a beam waist $w_0 = 5.7$ μm and a Rayleigh distance $z_0 = 13.3$ mm. Such a high order gap allows the realization of several revivals at quite short distances, the first one located at 3.55 mm and the second one at 8.00 mm. For a more accurate description of the pattern evolution, we scanned the transverse intensity distribution along a beam diameter at different propagation planes and displayed the corresponding 3D plot at the top graph in Fig. 4. Two revival positions can be clearly seen in the measured interval. We have also displayed the corresponding

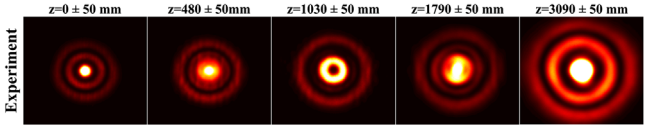

FIG. 5. Experimental results for the long range revival of the structured spot given by Eq. (21). The first revival occurs around 3.09 m from the initial plane.

theoretical result at the bottom graph. In both graphs, the intensity is normalized by the peak value at $x = 0$, $z = 0$. The average discrepancy between theoretical and experimental results (as measured by the ratio between the intensity difference and the theoretical value) is 2% over the entire xz domain covered by the graphs. It becomes more important where the intensity is small and the experimental result is more sensitive to the background noise.

In between two consecutive revivals, a dark spot is produced. This can be useful in tweezing applications where one desires to study the interaction between trapped particles and a surface or structure on which light incidence is to be avoided. In this case, the interacting structure can be placed at the dark spot close to the trapping bright region.

Finally, we have also measured pattern revival in the long distance range. For this end, we have employed the superposition

$$\psi_{\text{long}}(\mathbf{r}) = v_{0,0}(\mathbf{r}) + v_{3,0}(\mathbf{r}), \tag{21}$$

with a larger beam waist $w_0 = 600$ μm. This resulted in the largest structure allowed by the SLM screen. In contrast with the previous case, the longer Rayleigh distance $z_0 = 1.79$ m and the smaller mode gap produced the first revival at a distance around 3.09 m, therefore 3 orders of magnitude larger. The experimental result is shown in Fig. 5. As in the previous cases, we verified that the corresponding theoretical images agree with the measured ones within 2% discrepancy in average. Longer distances can be attained with specially designed masks with larger dimensions than those of the SLM screen, what can be useful for optical communication systems.

In conclusion, we have demonstrated a method for structuring light with pattern revivals using Gouy phase synchronization at fractional values. The propagation positions of the revivals are determined by the integer relation between the Gouy phase and the paraxial mode order, where commensurability between the different modes plays an essential role. This can motivate the quest for more involved connections between number theory and paraxial optics [33]. The ability to shape the transverse intensity distribution and address the beam energy to specific points without the need of intermediate optical components can be useful for free space communication and optical tweezing. Moreover, the Gouy phase plays also an important role in matter waves, where the ideas presented here can find interesting applications in electron beam microscopy and Bose-Einstein condensates.

Funding was provided by Coordenação de Aperfeiçoamento de Pessoal de Nível Superior (CAPES), Fundação Carlos Chagas Filho de Amparo à Pesquisa do Estado do Rio de Janeiro (FAPERJ), and Instituto Nacional de Ciência e Tecnologia de Informação Quântica (Grant No. CNPq INCT-IQ 465469/2014-0).

*Corresponding author.
azkhoury@id.uff.br

[1] S. P. Walborn, C. H. Monken, S. Pádua, and P. H. Souto Ribeiro, Phys. Rep. **495**, 87 (2010).
[2] M. J. Padgett, Opt. Express **25**, 11265 (2017).
[3] T. B. Pittman, Y. H. Shih, D. V. Strekalov, and A. V. Sergienko, Phys. Rev. A **52**, R3429 (1995).
[4] C. H. Monken, P. H. Souto Ribeiro, and S. Pádua, Phys. Rev. A **57**, 3123 (1998).
[5] E. J. S. Fonseca, P. H. Souto Ribeiro, S. Pádua, and C. H. Monken, Phys. Rev. A **60**, 1530 (1999).
[6] A. Valencia, G. Scarcelli, M. D'Angelo, and Y. Shih, Phys. Rev. Lett. **94**, 063601 (2005).
[7] B. I. Erkmen and J. H. Shapiro, Phys. Rev. A **77**, 043809 (2008).
[8] Y. Bromberg, O. Katz, and Y. Silberberg, Appl. Phys. Lett. **95**, 131110 (2009).
[9] D. S. Tasca, R. S. Aspden, P. A. Morris, G. Anderson, R. W. Boyd, and M. J. Padgett, Opt. Express **21**, 30460 (2013).
[10] D. Pelliccia, A. Rack, M. Scheel, V. Cantelli, and D. M. Paganin, Phys. Rev. Lett. **117**, 113902 (2016).
[11] H. Yu, R. Lu, S. Han, H. Xie, G. Du, T. Xiao, and D. Zhu, Phys. Rev. Lett. **117**, 113901 (2016).
[12] M. J. Padgett and R. W. Boyd, Phil. Trans. R. Soc. A **375**, 20160233 (2017).
[13] P. A. Moreau, E. Toninelli, T. Gregory, and M. J. Padgett, Laser Photonic Rev. **12**, 1700143 (2018).
[14] S. Li, F. Cropp, K. Kabra, T. J. Lane, G. Wetzstein, P. Musumeci, and D. Ratner, Phys. Rev. Lett. **121**, 114801 (2018).
[15] L. Neves, G. Lima, E. J. S. Fonseca, L. Davidovich, and S. Pádua, Phys. Rev. A **76**, 032314 (2007).
[16] I. Rodrigues, O. Cosme, and S. Pádua, J. Phys. B **43**, 125505 (2010).
[17] A. Z. Khoury, L. E. Oxman, B. Marques, A. Matoso, and S. Pádua, Phys. Rev. A **87**, 042113 (2013).
[18] J. Courtial, Opt. Commun. **151**, 1 (1998).
[19] S. M. Baumann, D. M. Kalb, L. H. MacMillan, and E. J. Galvez, Opt. Express **17**, 9818 (2009).
[20] H. F. Talbot, London Edinburgh Dublin Philos. Mag. J. Sci. **9**, 401 (1836).
[21] M. S. Chapman, C. R. Ekstrom, T. D. Hammond, J. Schmiedmayer, B. E. Tannian, S. Wehinger, and D. E. Pritchard, Phys. Rev. A **51**, R14 (1995).
[22] J. A. Yeazell, M. Mallalieu, and C. R. Stroud, Phys. Rev. Lett. **64**, 2007 (1990).
[23] F. W. Cummings, Phys. Rev. **140**, A1051 (1965).
[24] P. Meystre, E. Geneux, A. Quattropani, and A. Faist, Nuovo Cimento B **25**, 521 (1975).
[25] N. B. Narozhny, J. J. Sanchez-Mondragon, and J. H. Eberly, Phys. Rev. A **23**, 236 (1981).
[26] G. Rempe, H. Walther, and N. Klein, Phys. Rev. Lett. **58**, 353 (1987).
[27] K. Patorsky, in *The Self-Imaging Phenomenon and its Applications*, Progress in Optics XXVII, edited by E. Wolf (Elsevier Science Publishers B. V., Amsterdam, 1989).
[28] B. P. S. Ahluwalia, X-C. Yuan, and S. H. Tao, Opt. Commun. **238**, 177 (2004).
[29] J. Courtial, G. Whyte, Z. Bouchal, and J. Wagner, Opt. Express **14**, 2108 (2006).
[30] H. E. Kondakci and A. F. Abouraddy, Phys. Rev. Lett. **120**, 163901 (2018).
[31] L. E. Oxman and A. Z. Khoury, Phys. Rev. Lett. **106**, 240503 (2011).
[32] See Supplemental Material at http://link.aps.org/supplemental/10.1103/PhysRevLett.124.033902 for details on (i) theoretical animation of the structured spot evolution together with the phasors representing the individual Gouy phases. Revivals occur where the phasors line up, (ii) experimental animation of the UFF pattern propagation without noise filtering, and (iii) experimental animation of the UFF pattern propagation with noise filtering.
[33] S. Wolk, W. Merkel, W. P. Schleich, I. S. Averbukh, and B. Girard, New J. Phys. **13**, 103007 (2011).